The Astrophysical Journal, 575:996–1006, 2002 August 20
© 2002. The American Astronomical Society. All rights reserved. Printed in U.S.A.

DISCOVERY OF A BLACK HOLE MASS-PERIOD CORRELATION IN SOFT X-RAY TRANSIENTS AND ITS IMPLICATION FOR GAMMA-RAY BURST AND HYPERNOVA MECHANISMS

C.-H. Lee,[1,2,3] G. E. Brown,[3] and R. A. M. J. Wijers[3,4]
Received 2001 October 17; accepted 2002 April 23

ABSTRACT

We investigate the soft X-ray transients with black hole primaries, which may have been the sources of gamma-ray bursts (GRBs) and hypernovae earlier in their evolution. For systems with evolved donors, we are able to reconstruct the pre-explosion periods and find that the black hole mass increases with the orbital period of the binary. This correlation can be understood in terms of angular momentum support in the helium star progenitor of the black hole, if the systems with shorter periods had more rapidly rotating primaries prior to their explosion; centrifugal support will then prevent more of its mass from collapsing into the black hole on a dynamical time. This trend of more rapidly rotating stars in closer binaries is usual in close binaries and in the present case can be understood in terms of spin-up during spiral-in and subsequent tidal coupling. We investigate the relation quantitatively and obtain reasonable agreement with the observed mass-period correlation. An important ingredient is the fact that the rapidly rotating new black hole powers both a GRB and the hypernova explosion of the remaining envelope, so that the material initially prevented from falling into the black hole will be expelled rather than accreted. For systems in which the donor is now and will remain in main sequence, we cannot reconstruct the pre-explosion period in detail, because some of their history has been erased by angular momentum loss through magnetic braking and gravitational waves. We can, however, show that their periods at the time of black hole formation were most likely 0.4–0.7 days, somewhat greater than their present periods. Furthermore, their black holes would have been expected to accrete $\sim 1\ M_\odot$ of material from the donor during their previous evolution. Comparison with predictions suggests that little mass will be lost in the explosion for the relatively high pre-explosion periods of these binaries. A natural consequence of the He star rotation is that black holes formed in the shorter period (before explosion) soft X-ray transients acquire significant Kerr parameters. This makes them good sources of power for GRBs and hypernovae, via the Blandford-Znajek mechanism, and thus supports our model for the origin of GRBs in soft X-ray transients.

Subject headings: accretion, accretion disks — binaries: close — black hole physics — gamma-rays: bursts

1. INTRODUCTION

Recent observations strongly suggest a connection between gamma-ray bursts (GRBs) and supernovae, with indications that the supernovae in question are especially energetic and of Type Ib/c, i.e., core collapses of massive stars that have lost their hydrogen envelope (see van Paradijs, Kouveliotou, & Wijers 2000 and references therein). This supports suggestions by Woosley (1993) and Paczyński (1998) for the origin of GRBs in stellar core collapses. The hydrodynamics of a jet escaping from a star and causing its explosion was explored in detail by MacFadyen & Woosley (1999), who showed that contrary to accepted wisdom, a fairly baryon-free, ultrarelativistic jet could plow through the collapsing star and emerge with large Lorentz factors. The powering of the outflow by coupling of high magnetic fields to the rotation of the black hole (Blandford & Znajek 1977), first suggested by Paczyński (1998) in the context of GRBs, was worked out in detail by van Putten (1999, 2001). Li has also discussed the deposition of energy from a black hole into the accretion disk in a recent series of papers (e.g., Li 2000a, 2000b, 2000c, 2000d, 2002).

Building on these thoughts, we have modeled both the powering of a GRB by black hole rotation and the stellar evolution pathways that set up favorable conditions for that mechanism (Brown et al. 2000). An essential ingredient in this model is a rapidly rotating black hole, and it is this aspect that we focus on in the present paper. A single star initially in uniform rotation will tend to develop a differential rotation, because the core contracts strongly during evolution, and angular momentum conservation will therefore increase its angular velocity. However, given enough time, viscous stresses will even out these differences, and thus the net result is a loss of angular momentum of the innermost regions of the star. Spruit & Phinney (1998) argued that magnetic-field–mediated coupling is strong enough in single stars during the giant phase to make the cores very slow; so slow, in fact, that they required an asymmetric kick in the birth of pulsars to get their spin frequencies up to observed values. Livio & Pringle (1998) subsequently used observations of novae to argue for a weaker coupling, but still their coupling strength would lead to spin energies of black holes that are negligible as power sources for GRBs.

However, as suggested by MacFadyen & Woosley (1999), a massive star in a close binary will spin faster for a number of reasons: first, when the hydrogen envelope is lifted off by spiral-in, it will cease to serve as a sink of angular momentum for the core. Second, the tidal friction concomitant to

[1] School of Physics, Seoul National University, Seoul 151-747, Korea; chlee@kias.re.kr.
[2] School of Physics, Korea Institute for Advanced Study, Seoul 130-012, Korea.
[3] Department of Physics and Astronomy, State University of New York, Stony Brook, NY 11794; popenoe@nuclear.physics.sunysb.edu, rwijers@mail.astro.sunysb.edu.
[4] Current address: Astronomical Institute "Anton Pannekoek," University of Amsterdam, Kruislaan 403, 1098 SJ Amsterdam, The Netherlands; rwijers@science.uva.nl.

the spiral-in process will spin up the inner region, giving it a larger angular momentum than the same region in a single star (Rasio & Livio 1996). Third, tidal coupling in the close binary will tend to bring the primary into corotation with the orbital period. This latter process is not very efficient in the short post–spiral-in life of the binaries we consider, but its effect does probably matter to the outer layers of the helium star, which can be important for our work. With its more rapid rotation, the helium star then forms a black hole with a large Kerr parameter, which immediately after its formation (in a few seconds) begins to input power into its surroundings at a very high rate. This, then, powers both a GRB (e.g., Brown et al. 2000) and the expulsion of the material that was centrifugally prevented from falling into the black hole. In fact, van Putten (1999, 2001) estimates that the power input into that material exceeds that into the GRB, and Li (2000b) also finds that more energy can be extracted by the disk than by the GRB. It should be noted that an initially less rapidly rotating black hole could be spun up by disk accretion quite rapidly and start a similar process after some accretion has taken place (MacFadyen & Woosley 1999; Brown et al. 2000). Some implications of such more complicated sequences of events are discussed by Lee, Lee, & van Putten (2001).

In § 2 we present the data on known soft X-ray transients (SXTs), showing the relation between present orbital period and black hole mass. Since theory predicts a relation between pre-explosion orbital period and black hole mass, we then consider carefully the pre- and postexplosion evolution of the systems (§ 3) and use this to reconstruct the pre-explosion orbit for as many systems as possible (§ 4). Then we develop our model for the mass and spin of black holes in SXTs and use it to explain the mass-period correlation (§ 5). We summarize our conclusions in § 6.

2. AN EMPIRICAL CORRELATION BETWEEN ORBITAL PERIOD AND BLACK HOLE MASS

We have collected data from the literature on black hole binaries in our Galaxy. In Table 1, we collect data of those for which the mass function is known and some manner of mass estimate for both the black hole and the companion can be given. In Table 2, we list the properties of two key systems in more detail. In Figure 1, we show the masses of the black holes as a function of orbital period. While the ranges of black hole masses for main-sequence and evolved systems overlap, the latter tend to have higher masses; the exception is Nova Sco 1994, which we see later is a natural but rare case of the general evolution scenario that we describe in this paper. In Figure 2, we show the donor masses as a function of orbital period. They show a more obvious trend of more massive donors in evolved systems. As we see, this is a natural consequence of the fact that only evolved systems can come into Roche contact in wide binaries, and more massive donors are more likely to come into contact via nuclear evolution. (The various curves are explained in § 3.)

In the following sections, we argue that the correlation between black hole mass and period also has physical meaning: the shorter the orbital period, the more rapidly rotating the helium star progenitor to the black hole. Rapid rotation centrifugally prevents some fraction of the helium star from collapsing into a black hole, resulting in a smaller black hole mass. The correlation in Figure 1 is weak because evolution

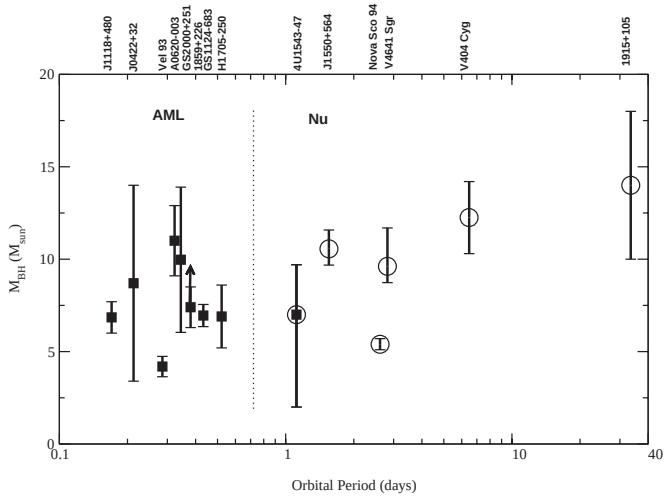

FIG. 1.—Black hole mass as a function of present orbital period of 14 SXTs. Note that the orbital period is on a logarithmic scale. SXTs with subgiant or giant companions are indicated by big open circles (denoted as "Nu" for nuclear evolution). Filled squares indicate SXTs with main-sequence companions (denoted as "AML" for angular momentum loss). The vertical dotted line indicates the possible existence of different classes according to evolutionary path of the binary, as discussed in § 3. 4U 1543−47 is marked with both symbols, since we believe it to be right on the borderline between main-sequence and evolved; for the purpose of modeling, it can be treated as evolved.

of the binary since formation of the black hole has washed out the relation. Properly, we should consider the correlation between pre-explosion orbital period and postexplosion black hole mass. Much of our work presented here is concerned with understanding the evolution of these binaries and using this knowledge to find the systems for which we can reconstruct those parameters. Using that subset, we show much better agreement between our model predictions and the observed relation between reconstructed period and mass; this supports our evolutionary model and has ramifications for the origin of GRBs.

3. THE EVOLUTION OF SOFT X-RAY TRANSIENTS

3.1. *Prior to the Formation of the Black Hole*

Following on the work of Brown, Weingartner, & Wijers (1996), who showed the importance of mass loss of helium stars in binaries in determining the final outcome of binary evolution, Brown, Lee, & Bethe (1999), Wellstein & Langer (1999), and Brown et al. (2001a) showed that massive helium stars could evolve into high-mass black holes only if they were covered with hydrogen during most of their helium core burning era (case C mass transfer in binaries). In cases A or B mass transfer in binaries (Roche lobe overflow in main-sequence or red giant stage), the Fe core that was left was too low in mass to go into a high-mass black hole. Brown et al. (2001a) showed that high-mass black holes could be formed only if the mass was taken off the black hole progenitor after helium core burning was finished; i.e., case C mass transfer. Brown, Lee, & Tauris (2001c) showed that with the Schaller et al. evolution, this could happen only in the neighborhood of zero-age main sequence (ZAMS) mass 20 $M_\odot$, definitely not at 25 $M_\odot$ and higher; because of the wind losses, the mass transfer would begin as Roche lobe overflow only in case B mass transfer,

TABLE 1

PARAMETERS OF BLACK HOLE BINARIES IN OUR GALAXY WITH MEASURED MASS FUNCTIONS

X-Ray Name	Companion Type	P_{orb} (day)	K_{opt} (km s^{-1})	$f(M_X)$ ($M_\odot$)	i (deg)	M_{BH} ($M_\odot$)	M_{opt} ($M_\odot$)	d (kpc)	Other Name(s)	References
XTE J1118+480	K7 V–M0 V	0.169930(4)	701(10)	6.1(3)	81(2)	6.0–7.7	0.09–0.5	1.9(4)	KV Ursae Majoris	1, 2
XN Per 92	M0 V	0.2127(7)	380.6(65)	1.15–1.27	28–45	3.4–14.0	0.10–0.97	...	GRO J0422+32, V518 Persei	3
XN Vel 93	K6–M0	0.2852	475.4(59)	3.05–3.29	~78	3.64–4.74	0.50–0.65	...	MM Velorum	4
XN Mon 75.....	K4 V	0.3230	433(3)	2.83–2.99	40.75(300)	11.0(19)	0.68(18)	1.164(114)	A0620−003, V616 Monocerotis, N Mon 1917	3, 5
XN Vul 88.....	K5 V	0.3441	520(16)	5.01(12)	47–75	6.04–13.9	0.26–0.59	2	GS 2000+251, QZ Vulpeculae	3, 6
XTE 1859+226	...	0.380(3)	570(27)	7.4(11)	...	...	...	...	V406 Vulpeculae	7
XN Mus 91	K4 V	0.4326	406(7)	2.86–3.16	54.0(15)	6.95(6)	0.56–0.90	3.0	GS 1124−683, GU Muscae	3, 8
XN Oph 77.....	K3 V	0.5213	420(30)	4.44–4.86	60–80	5.2–8.6	0.3–0.6	5.5	H1705−250, V2107 Ophiuchi	3
4U 1543−47.....	A2 V	1.1164	129.6(18)	0.252(11)	~22	2.0–9.7	1.3–2.6	9.1(11)	MX 1543−475, IL Lupi	9, 10
XTE J1550−564.....	G8 IV–K4 III	1.552(10)	349(12)	6.86(71)	70.8–75.4	$10.56^{+1.02}_{-0.88}$	$1.31^{+0.33}_{-0.37}$	4.7–5.9 (?)	V381 Normae	11
XN Sco 94.....	F6 III	2.6127(8)	227(2)	2.64–2.82	67–71	5.1–5.7	1.1–1.8	3.2	GRO J1655−40, V1033 Scorpii	3, 12
V4641 Sagittarii	B9 III	2.817	211.0(31)	2.74(12)	...	$9.61^{+2.08}_{-0.88}$	$6.53^{+1.6}_{-1.03}$	$9.59^{+2.72}_{-2.19}$	XTE J1819−254, SAX J1819.3−2525	13
Cyg X-1	O9.7 Iab	5.5996	74.7(10)	0.25(1)	...	~10.1	~17.8	2.5	1956+350, V1357 Cyg, HDE 226868	14
XN Cyg 89	K0 IV	6.4714	208.5(7)	6.02–6.12	52–60	10.3–14.2	0.57–0.92	2.2–3.7	GS 2023+338, V404 Cygni, N Cyg 1938, 1959	3, 15, 16
GRS 1915+105.....	K–M III	33.5(15)	140(15)	9.5(30)	70(2)	14(4)	1.2(2)	12.1(8)	V1487 Aquilae	17

NOTE.—Binaries are listed in order of increasing orbital period. All systems except Cyg X-1 (steady X-ray source) are SXTs. XN indicates X-ray nova. Earlier observations (Greene, Bailyn, & Orosz 2001) gave the black hole mass in Nova Sco as 6.3 ± 0.5 $M_\odot$ New analyses of the light curve by Beer & Podsiadlowski 2002 give a somewhat smaller mass 5.4 ± 0.3 $M_\odot$ and 1.45 ± 0.35 $M_\odot$ for the companion.

REFERENCES.—(1) McClintock et al. 2001; (2) Wagner et al. 2001; (3) Bailyn et al. 1998; (4) Filippenko et al. 1999; (5) Gelino et al. 2001b; (6) Harlaftis, Horne, & Filippenko 1996; (7) Filippenko & Chornock 2001; (8) Gelino et al. 2001a; (9) Orosz et al. 1998; (10) Orosz 2002; (11) Orosz et al. 2002; (12) Beer & Podsiadlowski 2002; (13) Orosz et al. 2001; (14) Herrero et al. 1995; (15) Shahbaz et al. 1994; (16) Shahbaz et al. 1996; (17) Greiner et al. 2001.

TABLE 2

PARAMETERS FOR NOVA SCORPII (BEER & PODSIADLOWSKI 2002) AND V4641 SGR (OROSZ ET AL. 2001)

Parameter	Nova Scorpii	V4641 Sgr
Orbital period (days)	2.623	2.817
Black hole mass ($M_\odot$)	5.4 ± 0.3	$9.61^{+2.08}_{-0.88}$
Companion mass ($M_\odot$)	1.45 ± 0.35	$6.53^{+1.6}_{-1.03}$
Total mass ($M_\odot$)	6.85	$16.19^{+3.58}_{-1.94}$
Mass ratio	0.27	1.50 ± 0.13
Orbital separation ($R_\odot$)	15.2	$21.33^{+1.25}_{-1.02}$
Companion radius ($R_\odot$)	4.15	$7.47^{+0.53}_{-0.47}$
Distance (kpc)	3.2	$9.59^{+2.72}_{-2.19}$

with these higher main-sequence masses, because the giant radii of these stars exceed their radii in the supergiant phase. Below we see that the high black hole masses in a few binaries require us to extend the range upward to about 30 $M_\odot$.

A major uncertainty in the evolution of all compact X-ray binaries is the phase of spiral-in that occurred in their evolution; these binaries are initially very wide, and when the primary fills its Roche lobe and transfers mass to the secondary, the mass transfer leads to instability, resulting in the secondary plunging into the primary's envelope. Next, dissipation of orbital energy of the secondary causes the primary's envelope to be ejected and the orbit to shrink. Following the original work by Webbink (1984), Brown et al. (2001c) write the standard formula for common-envelope evolution as

$$\frac{GM_pM_e}{\lambda R} = \frac{GM_pM_e}{\lambda r_L a_i} = \alpha_{\rm ce}\left(\frac{GM_{\rm He}M_d}{2a_f} - \frac{GM_pM_d}{2a_i}\right), \quad (1)$$

where M_p is the total mass of the black hole progenitor star just before the common envelope forms, M_e is the mass of its hydrogen envelope, $M_{\rm He}$ is the mass of its core, a_i and a_f are the initial and final separation, before and after the common envelope, respectively, and $r_L \equiv R_L/a$ is the dimensionless Roche lobe radius. This equation essentially relates the loss of orbital energy of the secondary to the binding energy of the ejected envelope. The parameter λ is a shape parameter for the density profile of the envelope. It can vary greatly between stars (Tauris & Dewi 2001), but for the extended, deeply convective giants we deal with in case C mass transfer, it is always close to 7/6. (See also Appendix C of Brown et al. 2001b.) The parameter $\alpha_{\rm ce}$ accounts for the efficiency with which orbital energy is used to expel the envelope, and may also account for some other effects such as extra energy sources and the possibility that each mass element of the envelope receives more than the minimum energy needed to escape (see, e.g., Bhattacharya & van den Heuvel 1991 and references therein).

Given the parameters of the system at first Roche contact, when spiral-in starts, the final separation is determined by the product of λ and $\alpha_{\rm ce}$, the efficiency of the energy conversion. In general, these parameters are only the simplest recipe prescription for the complex hydrodynamical interaction during spiral-in. While we therefore cannot predict the value of $\lambda\alpha_{\rm ce}$ from first principles, we can try to find its value from constraints in some systems and then assume it is the same for all similar systems. Brown, Lee, & Tauris found a great regularity in the evolution of SXTs with main-sequence companions, all but one of which are K or M stars, which constrained the efficiency $\lambda\alpha_{\rm ce}$ to be 0.2–0.5. However, these authors did not include mass loss in the explosion, which we do here in our evolution of SXTs with evolved companions. Since mass loss substantially widens the orbits, including it the common-envelope evolution must bring the (pre-explosion) a_f to a smaller value: if $M_{\rm post}$ is the black hole plus companion mass and ΔM the mass lost in the formation of the black hole, we have

$$a_{f,\,\rm post} = a_{f,\,\rm pre}(1 + \Delta M/M_{\rm post}) \quad (2)$$

(after the orbit has been recircularized). Therefore, there has been an extra widening since the explosion by a factor of up to about 1.5. We found $\lambda\alpha_{\rm ce}$ to be in the lower part of the interval found by Brown et al. (2001c), $\lambda\alpha_{\rm ce} \sim 0.2$.

We can achieve a more precise "calibration" of the value of $\lambda\alpha_{\rm ce}$ if we manage to find some systems in which we can estimate both the initial and the final separation. To estimate the initial separation (at the onset of spiral-in), we need to know the mass and radius of the black hole progenitor and combine this with the Roche lobe–filling condition. The helium star progenitors in at least three of the evolved binaries seem to be too massive for the 20–23 $M_\odot$ ZAMS progenitors used by Brown et al. (2001c); the black hole in V404 Cyg is probably at least 10 $M_\odot$ (Shahbaz et al. 1994,

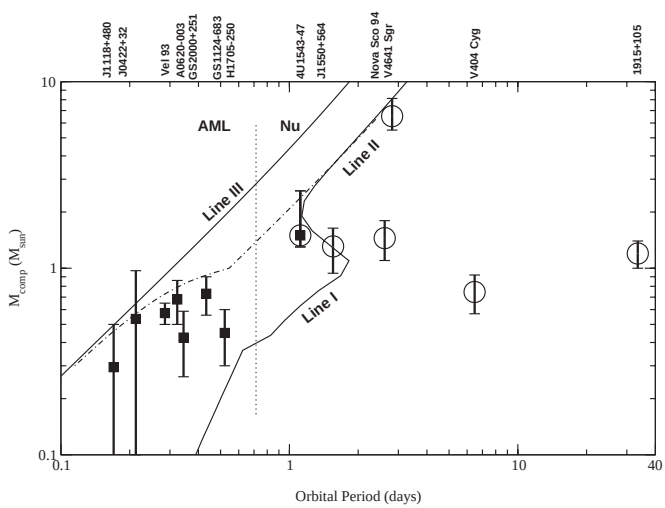

FIG. 2.—Companion mass as a function of present orbital period of 13 SXTs. XTE 1859+226 is not included because the companion mass is not well determined (Filippenko & Chornock 2001). Symbols of SXTs are the same as in Fig. 1. Line III indicates the orbital period for which a companion of that mass fills its Roche lobe on the ZAMS. No system can exist above and to the left of this line for a significant duration. Lines I and II are the upper-period limit for systems that can come into contact while the donor is on the main sequence. For high masses (line II), this limit is set by the period at which the evolution time of the companion is too short to allow the orbit to shrink significantly before it leaves the main sequence. For low masses (line I), where the donor never evolves off the main sequence within a Hubble time, the limit is set by the period for which the shrinking timescale of the orbit equals the Hubble time. The dot-dashed line indicates the point at which a system that starts its life on lines I/II comes into Roche contact. For very low masses, this equals line III, because the donor never moves significantly away from its ZAMS radius, whereas for very high masses it equals line II, because the orbit cannot shrink before the companion evolves off the main sequence. At intermediate masses, the companion expands somewhat, while the orbit shrinks and fills its Roche lobe at a larger period than line III. Systems that become SXTs with main-sequence donors within a Hubble time must start between line III and line I/II. At the start of mass transfer, they must lie in the narrow strip between line III and the dot-dashed line.

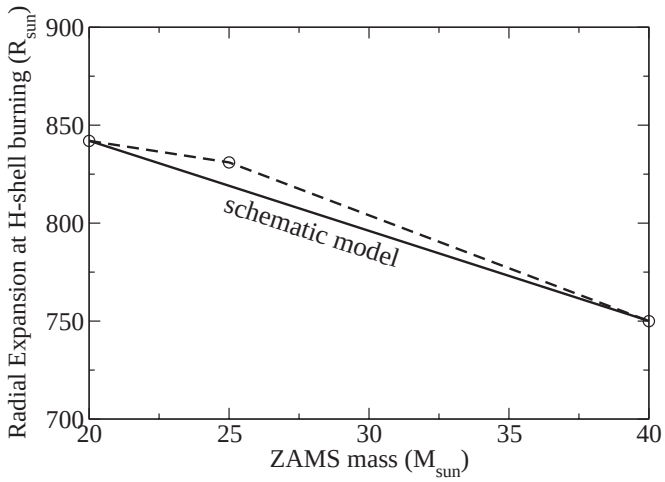

FIG. 3.—Radial expansion at the end of the giant branch. The data are taken from Schaller et al. (1992). Radial expansions are 842, 831, and 750 $R_\odot$ for 20, 25, and 40 $M_\odot$, respectively. The radial expansion shows an almost linear dependence on the ZAMS mass.

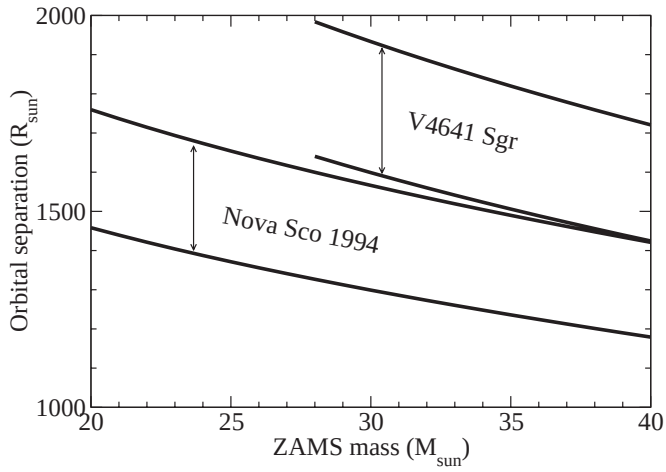

FIG. 4.—Possible initial orbital separations for case C mass transfer with 1.91 $M_\odot$ (Nova Sco) and 6.53 $M_\odot$ (V4641 Sgr) main-sequence companions. For Nova Sco, the estimated companion mass 1.91 $M_\odot$ during the common-envelope evolution is used as discussed in § 3. The x-axis is the ZAMS mass of the black hole progenitor.

1996; Bailyn et al. 1998), and the black hole in Nova Scorpii is of mass ~5.4 ± 0.3 $M_\odot$ (Beer & Podsiadlowski 2002), and the mass loss in black hole formation is $\gtrsim 5$ $M_\odot$ (Nelemans, Tauris, & van den Heuvel 1999), so that the progenitor of the helium star must have been ~11 $M_\odot$. From Table 2, the black hole in V4641 Sgr is of mass $9.61^{+2.08}_{-0.88}$ $M_\odot$ (Orosz et al. 2001). The tentative conclusion from the above is that at least these binaries with evolved companions seem to have come from helium cores of ~11 $M_\odot$ or ZAMS mass ~30 $M_\odot$. With high wind mass-loss rates as proposed by Schaller et al. (1992), such massive stars have larger radii as giants than as supergiants, thus making case C mass transfer impossible. However, since radii and mass-loss rates of evolved stars are very uncertain, we take the view that the need for ~11 $M_\odot$ helium cores implies that their progenitors, 30 $M_\odot$ main-sequence stars, do expand enough to allow case C mass transfer.

In Figure 3, we summarize the radius at the end of the giant branch as a function of ZAMS mass (Schaller et al. 1992). The ZAMS mass dependence of this final giant radius is adequately represented by a linear function in the region of 20–40 $M_\odot$. We assume that the radial expansion during the helium burning can be scaled to the case of a 20 $M_\odot$ star using this linear relation as follows:

$$R(M;t) = \left[-\frac{842\ R_\odot - 750\ R_\odot}{842\ R_\odot}\frac{(M - 20\ M_\odot)}{20\ M_\odot} + 1\right] \times R(20\ M_\odot; t)\ . \quad (3)$$

Further, we took the mass-loss rate of 20 $M_\odot$ as standard and scaled the mass-loss rate in proportion to the ZAMS mass. The allowed range of case C mass transfer with ZAMS mass 20 $M_\odot$ is 971 $R_\odot < R < 1185$ $R_\odot$, that of Schaller et al. (1992). In Figure 4 are given the possible initial orbital separations for case C mass transfer for the 1.91 $M_\odot$ companion appropriate for Nova Sco (see § 4) and for the 6.53 $M_\odot$ companion appropriate for V4641 Sgr (Orosz et al. 2001).

Now if we look at equation (1), we see that a_f scales almost linearly with the donor (companion) mass M_d. The envelope mass M_e is roughly 0.7 $M_{\rm giant}$ (Bethe & Brown 1998), and we use

$$M_{\rm He} = 0.08(M_{\rm giant}/M_\odot)^{1.45} M_\odot\ , \quad (4)$$

so that

$$a_f \propto \frac{M_d}{M_\odot}\left(\frac{M_{\rm giant}}{M_\odot}\right)^{-0.55} a_i\ , \quad (5)$$

assuming $\lambda\alpha_{\rm ce}$ to be constant and with neglect of the small term in a_i^{-1} in the right-hand side of equation (1). From our curves (Fig. 4), we see that the 20% possible variation in a_i results in the same percentage variation in a_f. Because the actual ZAMS mass can be anywhere in the range 20–30 $M_\odot$, there can be an additional ~25% variation in a_f with giant mass, as compared with the linear dependence on M_d. In view of the modest size of these variations at a given donor mass, we make the approximation in the rest of the paper that the pre-explosion orbital separation depends only on M_d and scales linearly with M_d. This simple scaling and the modest amount of scatter around it are partly the result of the weak dependences on initial parameters in equation (5) but chiefly the result of the fact that our model uses case C mass transfer. This constrains the Roche contact to first occur when the radius of the star is in a very narrow range, between the maximum radius in the giant phase and the maximum radius in the supergiant phase.

To complete our calibration of the spiral-in efficiency, we must find systems in which we can also estimate the orbital separation just after spiral-in well. This is complicated by the fact that mass transfer has taken place since the spiral-in. Most SXTs have small mass ratios, and for such small mass ratios the orbital separation is fairly sensitive to the amount of mass transferred, making it hard to derive the post–spiral-in separation from the present one. The exception is V4641 Sgr, in which the present mass ratio is close to 1. Since the initial mass ratio could not have been significantly greater than 1 (since that would result in unstable mass transfer), and furthermore the orbital period changes very little with mass transfer for nearly equal masses, we can fairly approximate the post–spiral-in separation by the

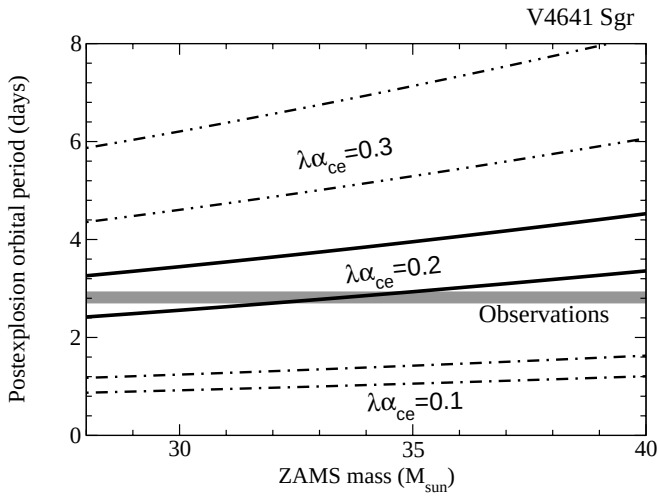

FIG. 5.—Postexplosion orbital periods of V4641 Sgr after black hole formation for various common-envelope efficiencies. The x-axis is the ZAMS masses of black hole progenitor. The width of each band is determined by the initial band of possible case C mass transfer given in Fig. 4. Here $\lambda\alpha_{\rm ce} \sim 0.2$ is consistent with current observations.

present one. In Figure 5, we show the predicted ranges of post–spiral-in orbital periods for different values of $\lambda\alpha_{\rm ce}$. Clearly, a value quite close to 0.2 is indicated. For 4U 1543−47 (IL Lupi), we find that it is near the boundary between evolved and main-sequence evolution. To place it there, as discussed in § 4, we find from the reconstructed orbital period in Figure 6 that $\lambda\alpha_{\rm ce} \sim 0.2$ is also consistent with the properties of this system.

In short, the general properties of SXTs and the specific cases of V4641 Sgr and IL Lup favor $\lambda\alpha_{\rm ce} \sim 0.2$, which we therefore adopt as a general efficiency for the evolution of other transient sources. This then makes it possible to make quite specific predictions for the prior evolution of many of the other SXTs.

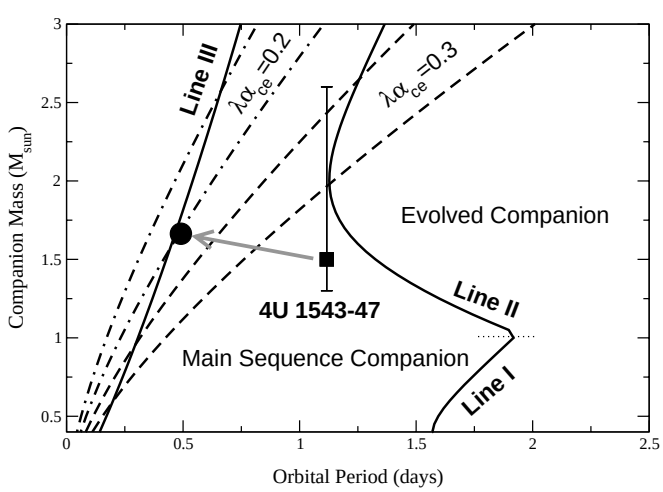

FIG. 6.—Enlargement of the central region of Fig. 2, indicating the present location of IL Lup. If we adopt the same value $\lambda\alpha_{\rm ce} = 0.2$ for the common-envelope parameter, we see that the reconstructed post–spiral-in period places the system right on the main-sequence line, implying a fairly tight constraint on the initial parameters of this system. (We took the ZAMS mass of the black hole progenitor to be 30 $M_\odot$, which corresponds to $M_p \sim 25\ M_\odot$ in the beginning of case C mass transfer, and $M_{\rm He} = 11\ M_\odot$.)

3.2. *Expected Regularities*

From the above theory, certain regularities follow for the system behavior as a function of companion mass. First, the binding energy relation for spiral-in (eq. [1]) shows that very nearly $a_f \propto M_d$, with not much variation due to other aspects of the systems (see § 3.1). Furthermore, the relation between Roche lobe radius and donor mass when $M_d \ll M_{\rm BH}$ implies that $R_L/a_f \propto M_d^{1/3}$ (e.g., Eggleton 1983). As a result, the Roche lobe radius of the donor just after spiral-in will scale with donor mass as $R_L \propto M_d^{4/3}$. On the other hand, the donor radius itself depends on its mass only as $R_d \propto M_d^{0.8}$. Therefore, a low-mass donor overfills its Roche lobe immediately after spiral-in. In the donor mass range we consider ($M_d \gtrsim 0.7\ M_\odot$) it does not overfill its Roche lobe by much, so we assume that the system adjusts itself quickly by transfer of a small amount of mass to the He star, which widens the orbit until the donor fills its Roche lobe exactly. Above this minimum mass, there will be a range of donor masses that are close enough to filling their Roche lobes after spiral-in that they will be tidally locked and will come into contact via angular momentum loss (AML). Above this, there will be a range of mixed evolution, where both AML and nuclear evolution (Nu) play a role. Finally, for the most massive donors, $M_d > 2\ M_\odot$, the post–spiral-in orbits will be too wide for AML to shrink them much, so mass transfer will be initiated only via nuclear expansion of the donor. Of course, the ranges of case C radii of stars and variations of primary masses will ensure that the boundaries between these regions are not sharp; near the boundaries the fate of the system depends on its precise initial parameters.

4. RECONSTRUCTING THE PRE-EXPLOSION ORBITS

1. Nova Sco 94 (GRO J1655−40): The most extensive evolutionary studies have been made for Nova Sco. Starting from the work of Regős, Tout, & Wickramasinghe (1998), who make the case that the companion is in late main-sequence evolution, Beer & Podsiadlowski (2002) carry out extensive numerical calculations of the evolution, starting with a pre-explosion mass of 2.5 $M_\odot$ and separation of $\sim$6 $R_\odot$. More schematically, we arrived at a pre-explosion mass of 1.91 $M_\odot$ and separation of 5.33 $R_\odot$. We consequently have a 0.4 day pre-explosion period. With $\sim$6 $M_\odot$ mass loss in the explosion (Nelemans et al. 1999), nearly half the system mass, the binary period increases to 1.5 days, well beyond the period gap. This is also the period required if the common-envelope efficiency in this binary were again 0.2 (Fig. 7). This explains why Nova Sco is the only system with a giant donor and a black hole mass in the lower end of the range; its evolution really places it among the narrow-orbit systems. Generally, the mass loss during explosion is mild and does not change which category a system belongs to. But in those exceptional cases in which the mass loss comes close to half the total mass, the orbit widens very much and converts an AML system to a nuclear evolution system. We discuss in § 6 that help in expelling the mass may come from early onset of the GRB mechanism. After explosion, the binary evolves to its present period by nearly conservative mass transfer. Our estimate is that 0.41 $M_\odot$ is transferred from the donor to the black hole. Brown et al. (1999b) first made the case that Nova Sco was the relic of a GRB.

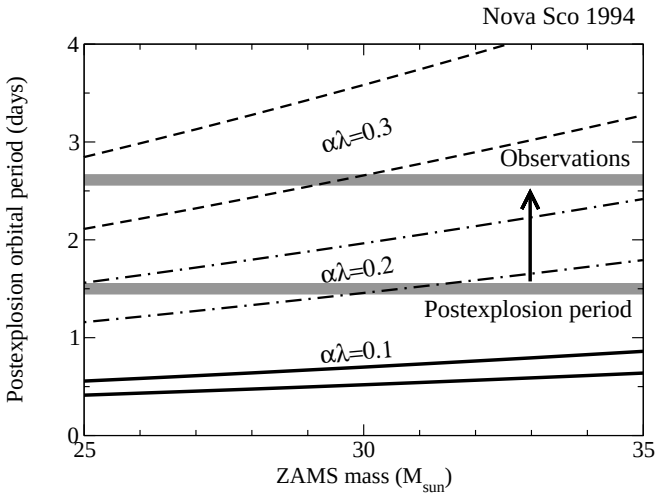

FIG. 7.—Postexplosion orbital periods of Nova Sco after black hole formation for various common-envelope efficiencies. For our calculation, we use a postexplosion black hole mass $M_{\rm BH} \sim 4.94\ M_\odot$ and a companion mass $M_d \sim 1.91\ M_\odot$. The x-axis is the ZAMS mass of black hole progenitor. The width of each band is determined by the initial band of possible case C mass transfer separations given in Fig. 4. A postexplosion period of about 1.5 days is consistent with $\lambda\alpha_{\rm ce} \sim 0.2$. By conservative mass transfer of 0.46 $M_\odot$ from the companion star to the black hole, the orbital period can be evolved to the currently observed orbital period.

2. V4641 Sgr: As we discussed in § 3, this system is our calibrator for the spiral-in efficiency, and we assume that its present state is very close to the one immediately following spiral-in.

3. GRS 1915+105: Recently, Greiner et al. (2001) determined the period and black hole mass of GRS 1915+105 to be 33.5 days and $14 \pm 4\ M_\odot$. Interestingly, we can evolve a system with properties very close to this by simply starting from V4641 Sgr and following its future evolution with conservative mass transfer ($P_{\rm orb} \propto \mu^3$, where μ is the reduced mass); allowing for 4.6 $M_\odot$ to be transferred from the donor to the black hole, we have

$$P_{1915} = \left(\frac{9.61 \times 6.53}{14.21 \times 1.93}\right)^3 P_{4641} = 33.7 \text{ days} . \qquad (6)$$

This would give a companion mass of 1.93 $M_\odot$, as compared with the Greiner et al. (2001) mass of $M_d = 1.2 \pm 0.2\ M_\odot$. However, the mass transfer cannot be completely conservative because of loss by jets, etc., as evidenced by the microquasar character of this object. Furthermore, the above M_d is viewed as a lower limit by Greiner et al. because the donor is being cooled by rapid mass loss, but its mass is estimated by comparison with noninteracting stars. We thus believe our evolution to be reasonable. We position the pre-explosion period and black hole mass of GRS 1915+105 at the same point as V4641 Sgr. Since mass transfer and widening of the orbit always occur together, the effect of this post-explosion evolution is to introduce a weak secondary correlation between orbital period and companion mass in the long-period regime, where such a correlation is not expected to arise from the pre-explosion evolution.

4. IL Lup: Recently, overabundances of Mg in the companion star of IL Lup have been observed (J. A. Orosz 2002, private communication). In analogy with the case of the overabundances in Nova Sco (Israelian et al. 1999; Brown et al. 2000), this indicates that there was an explosion at the time of black hole formation in this system, in which some of the material ejected from the core of the helium star progenitor to the black hole ended up on the companion. Based on these observations and our given efficiency $\lambda\alpha_{\rm ce} = 0.2$, one can start with the
11 $M_\odot$ He star and 1.7 $M_\odot$ companion as a possible progenitor of IL Lup. From the lower boundary of the curve with $\lambda\alpha_{\rm ce} = 0.2$ in Figure 6, the period would be 0.5 days. By losing 4.2 $M_\odot$ during the explosion, the binary orbit would be widened to 1.12 days. The period had to be shortened to 0.8 days by magnetic braking and gravitation wave radiation before the mass transfer started. Conservative transfer of 0.23 $M_\odot$ from the companion to the black hole would bring the period from 0.8 days to the present 1.1164 days.

5. V404 Cyg: The black hole in V404 Cyg appears to be somewhat more massive than in IL Lup, so we begin with a similar mass companion, but a 10 $M_\odot$ black hole, which would have a period of 0.63 days. Again, we neglect mass loss in the explosion, although a small correction for this might be made later. Conservative transfer of 1 $M_\odot$ from the donor to the black hole then brings the period to

$$0.63 \text{ days}\left(\frac{1.7\ M_\odot \times 10\ M_\odot}{0.7\ M_\odot \times 11\ M_\odot}\right)^3 = 6.7 \text{ days} , \qquad (7)$$

close to the present 6.47 day period. Here we take 11 and 0.7 $M_\odot$ as current masses in V404 Cyg (Orosz 2002). The black hole in V404 Cyg seems to be somewhat more massive than the others in the transient sources, with the exception of that in GRS 1915+105. In both cases, we achieve the relatively high black hole masses and periods by substantial accretion onto the black hole.

6. GRO J1550−564: The high-mass black hole in J1550−564, 10.56 $M_\odot$ (Orosz et al. 2002), is slightly less massive than the assumed black hole mass of V404 Cyg, and the companion is more massive than V404 Cyg with short period, 1.552 days. So, we start from the same initial conditions just derived for V404 Cyg (Fig. 11) and end up with the present system via simple conservative mass transfer.

7. Cygnus X-1: Cyg X-1 is usually not considered to have come from the same evolutionary path as the SXTs, since it is a persistent X-ray source with a much more massive donor. But with the discovery of objects with relatively massive donors in the SXT category, such as V4641 Sgr, it is worth considering the implications of our model for it. Cyg X-1 has been shown to have an appreciable system velocity (Kaper et al. 1999), although it may be only one-third the 50 km s^{-1} given there, depending on the O star association (L. Kaper 2001, private communication). The evolution of Cyg X-1 may have been similar to that of the transient sources, the difference being in the copious mass loss from the companion O9 I star, causing the black hole to accrete and emit X rays continuously. If we scale to Nova Sco to obtain the initial binary separation, we find

$$a_f = \frac{17.8\ M_\odot}{1.91\ M_\odot} \times 5.33\ R_\odot = 50\ R_\odot , \qquad (8)$$

somewhat larger than the present binary separation of 40 $R_\odot$. (We would obtain 38 $R_\odot$ if we scaled from the Beer & Podsiadlowski [2002] companion mass of 2.5 $M_\odot$ for Nova Sco.) Given uncertainties in the mass measurements, we believe it possible for Cyg X-1 to be accommodated in this scheme. Some sort of common-envelope evolution seems to

be necessary to narrow the orbit in the evolution involving the necessarily very massive progenitor stars (Brown et al. 2001a).

4.1. *Problems with the Close (AML) Systems*

Reconstruction of the AML binaries is more complicated, because they have lost angular momentum through magnetic braking and gravitational waves, so that their present positions as plotted in Figure 1 are not those at preexplosion time. As with the evolved companions, matter will have been accreted onto the black hole, so the black hole masses will be somewhat greater than just following the explosion. As noted earlier, the binaries with less massive companions with separation a_f at the end of common-envelope evolution overfill their Roche lobes. The outer part of the companion, down to the Roche lobe R_L, is transferred onto the He star. This mass transfer widens the orbit to R_L, possibly overshooting. Unless much mass is lost in the explosion when the black hole is formed, the Roche lobe radius is unchanged by the formation of the black hole and corresponds to line III in Figure 2.

Brown et al. (2001c) explored the evolution of ZAMS 1.25 $M_\odot$ stars under magnetic braking, gravitational waves, and mass transfer to the black hole. We adapt the same methods to make a more detailed study of the AML. First of all, we construct (Fig. 2) the lower limit on the companion mass for evolution in a Hubble time, giving the dashed line there. All binaries with companions in the main sequence at the beginning of mass transfer must lie between the dashed line and line III in that figure. The fact that the AMLs tend to lie below the dashed line implies both mass loss from the companion and accretion onto the black hole. Therefore, all these systems have shrunk their orbits and increased their black hole mass since the formation of the black hole by amounts that cannot be determined well. In Figure 10, however, we show where the four shortest period AMLs would have come from, had they lost 0.7 $M_\odot$ from an initial 1.5 $M_\odot$. From our earlier discussion about the a_f following common-envelope evolution, we saw that binaries with companions that stayed in the main sequence were favored to come from companion masses less than 2 $M_\odot$, and from Figure 2 we see that they would chiefly have companion ZAMS mass greater than $\sim$1 $M_\odot$, so that most of them would initially have periods of 0.4–0.7 days (which follows from the separations obtained from our eq. [5]). In trying to understand the detailed evolution of the AML, we begin from a binary with a 2 $M_\odot$ companion that just fills its Roche lobe following common-envelope evolution. We then follow its evolution under the two different assumptions made in Brown et al. (2001c): (1) that its time of evolution is always given by its initial 2 $M_\odot$ mass, i.e., ignoring effects of mass loss on the internal evolution time (Fig. 8, *dashed lines*, and Fig. 9, *right dashed line*), and (2) that the evolution of the star proceeds according to its adjusted mass (Fig. 8, *solid lines*, and Fig. 9, *left dashed line*). Since mass loss drives the companion out of thermal equilibrium, these two extremes bracket the outcome of a full stellar model calculation.

In summary, the AML systems have had the information on their postexplosion parameters partly erased by subse-

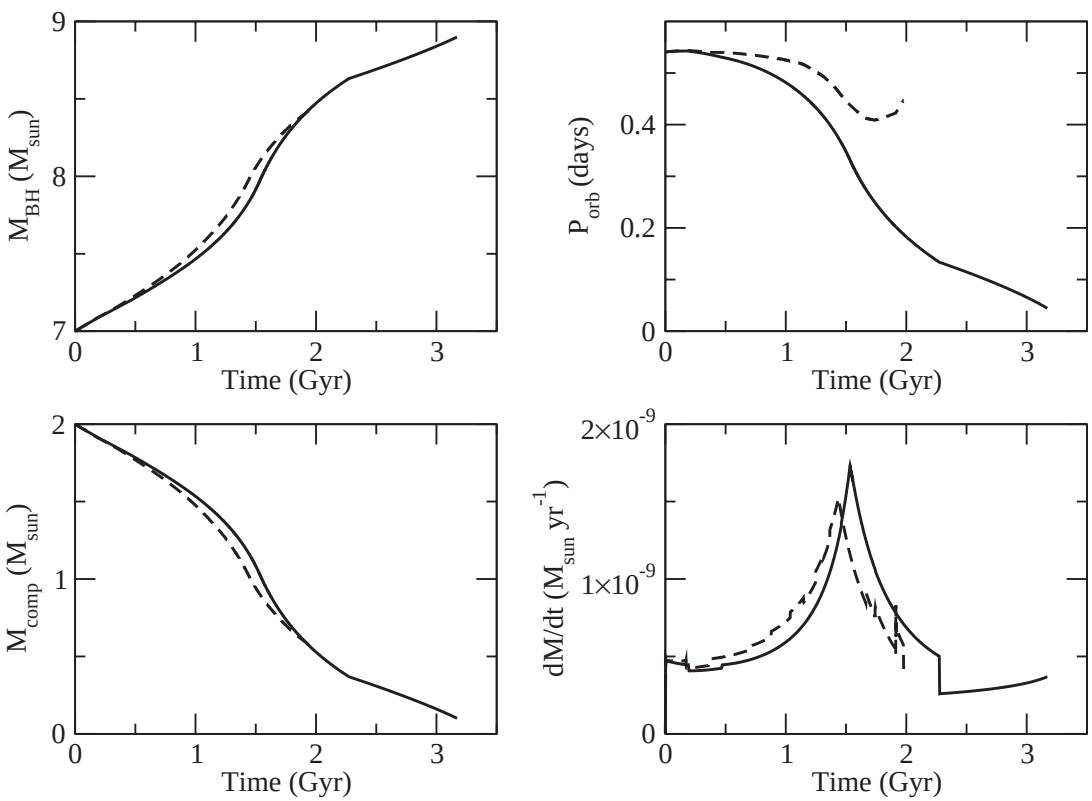

FIG. 8.—Evolution of a binary with 7 $M_\odot$ black hole and 2 $M_\odot$ companion for the initial period of 0.54 days. The solid line marks the evolution in case the companion star adjusts itself as it loses mass; the dashed line traces the evolution in case the mass loss does not affect the internal timescale of the companion star, so that it follows the same time evolution as an undisturbed 2 $M_\odot$ star.

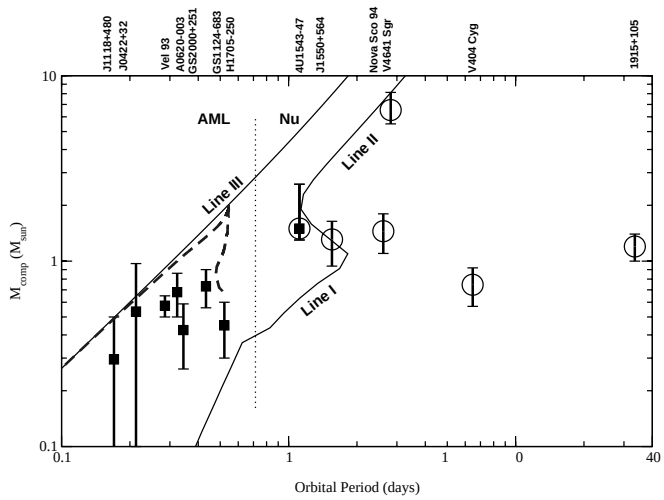

FIG. 9.—Evolutionary tracks of a binary with 9 $M_\odot$ black hole and 2 $M_\odot$ companion for the initial period of 0.54 days. The two evolution possibilities are as in Fig. 8. Left (right) dashed line corresponds to the solid (dashed) lines in Fig. 8.

quent evolution, in a manner that we cannot undo. Therefore, they can only provide a crude consistency check on the mass-period relation for black holes in SXTs, rather than provide precise constraints.

5. ANGULAR MOMENTUM AND ITS CONSEQUENCES FOR THE MASS AND SPIN OF THE BLACK HOLE

It is, in general, a difficult and unsolved problem to calculate the angular momentum of a stellar core at any given time. Even if we make the usual assumption that the rotation is initially solid body and not very far away from the maximal stable rotation frequency, the viscous coupling between the various layers of the star as it evolves is poorly known, and thus it is hard to be very quantitative. The general trend, however, is that the core will shrink and the envelope expand. In absence of viscous coupling, every mass element retains its angular momentum, and hence the core spins up as the envelope spins down, setting up a strong gradient in rotation frequency between the core and the envelope. Viscosity will then act to reduce this gradient, transporting angular momentum from the core to the envelope, but the efficiency of this process is very uncertain (Spruit & Phinney 1998; Livio & Pringle 1998).

As we noted in § 1, in our scenario, a number of effects will increase the angular momentum of the core relative to a similar core of a single star: (1) during spiral-in, the matter somewhat inside the orbit of the secondary is spun up by tidal torques (Rasio & Livio 1996), (2) the removal of the envelope halts the viscous slowdown of the core by friction with the envelope, and (3) during the post–spiral-in evolution, tidal coupling will tend to spin the helium star up even closer to the orbital period than was achieved by the first effect. This will not be a very strong effect because the duration of this phase is short, but it will affect the outer parts of the helium star somewhat, and this is the most important part (see below).

The net result of all these effects will be that the helium star will spin fairly rapidly, especially its envelope. The core is not so crucial to our argument about the fraction of the star that can fall into the black hole, since the few solar masses in it will not be centrifugally supported even in quite short orbits. For the purpose of a definite calculation, we therefore make the following assumptions: (1) the helium star corotates with the orbit before explosion and is in solid-body rotation, and (2) the mass distribution of the helium star with radius is given by a fully radiative zero-age helium main-sequence star. This latter approximation is, of course, not extremely good. However, what counts is the angular momentum as a function of mass, so the fact that the mass distribution has changed from helium ZAMS to explosion would be entirely inconsequential if no redistribution of angular momentum had taken place in the interim. As we saw above, any redistribution of angular momentum would take the form of angular momentum transport toward the outer layers. This means that relative to our ideal calculations below, a better calculation would find more angular momentum in the outer layers and therefore somewhat smaller black hole masses than the ones we calculate.

We now investigate how much mass will be prevented from falling into the black hole by the angular momentum of the He star, under the above assumptions of solid-body rotation with a period equal to that of the binary. If we assume that angular momentum is conserved during the collapse, we can get the cylindrical radius R_c, within which matter is not centrifugally prevented from falling into the black hole:

$$R_c^2\Omega = \tilde{l}(\hat{a})\,\frac{GM_c}{c}\ , \tag{9}$$

where $\tilde{l}(\hat{a})$ is the dimensionless specific angular momentum of the marginally bound orbit for a given Kerr parameter $\hat{a}$, and M_c is the total mass inside the cylinder of radius R_c. The Kerr parameter becomes

$$\hat{a} = \frac{I_c\Omega}{GM_c^2/c} = k^2\tilde{l}(\hat{a})\ , \tag{10}$$

where I_c is the total moment of inertia inside the cylinder of radius R_c, $I_c = k^2 M_c R_c^2$. Here M_c gives an estimate of the final black hole mass. Combining these relations with a profile of angular momentum and mass versus radius using the assumptions listed above, we can calculate the expected black hole mass and Kerr parameter as a function of SXT period before explosion.

In Figure 10, we show the predicted relation between orbital period and black hole mass for different helium star masses in our model. We compare these with the *present* properties of all SXTs for which the required parameters are known. The properties are consistent with the theoretical relations but do not confirm it very strongly because of the evolutionary changes discussed in § 4. Specifically, the AML systems lie above and to the left of the curves, because their orbits shrunk and their black holes accreted mass since the formation of the black hole. However, as we saw in § 4.1, plausible amounts of conservative mass transfer since the explosion would place the systems among the theoretical postexplosion curves (Fig. 10, *open squares and arrows*).

To test the theory more strongly, we show in Figure 11 only those systems for which the pre-explosion properties could be reconstructed (§ 4). We compare the observed points with ideal polytropic helium stars of 7 and 11 $M_\odot$ and with a full-model calculation obtained from Woosley

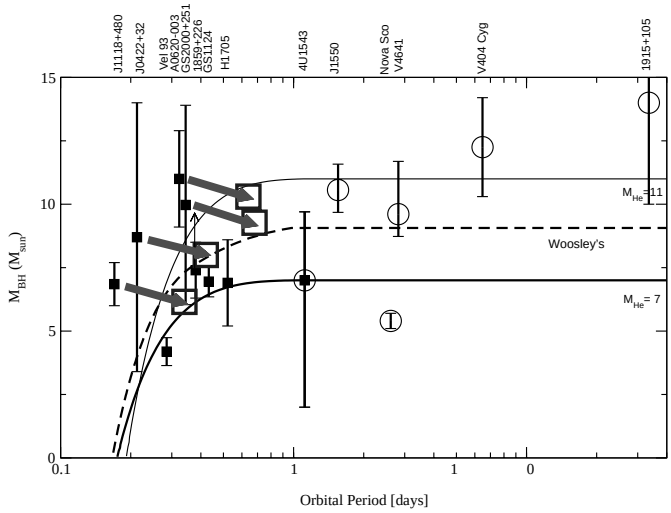

FIG. 10.—Present orbital period vs. black hole masses of SXTs. The deviations from the theoretical curves are substantial because of the post-explosion evolution of the binaries. The arrows on the AML systems point to an approximate postexplosion location if the donor mass was initially 1.5 $M_\odot$, and 0.7 $M_\odot$ has now been transferred to the black hole. The solid lines indicate the possible ranges of black hole masses with polytropic index $n = 3$ (radiative) for given pre-explosion spin periods that are assumed to be the same as the pre-explosion orbital period. Here we used $R_{\rm He} = 0.22(M_{\rm He}/M_\odot)^{0.6}\ R_\odot$. For comparison, the results with a "scaled" He core (9.15 $M_\odot$) of Woosley's 25 $M_\odot$ star at the beginning of ^{12}C burning with $T_c = 5 \times 10^8$ K, appropriate for case C mass transfer, are plotted as a dashed line (S. E. Woosley 2001, private communication). In this plot, we scaled the radius of Woosley's core, $R_{\rm Woosley} \sim 3 \times 10^{10}$ cm, by a factor of 2. As can be seen, the AML systems can plausibly originate from systems within the curves and thus are consistent with our theory. However, since they could have originated anywhere between the open square and their current location, they do not strongly test the theory.

(2001). By coincidence, the curves converge near the region of the shortest period observed systems, so that the uncertainty in helium star mass is not of great importance to the outcome. A helium star mass in the lower end of the range (7–9 $M_\odot$) may be somewhat preferred for these systems. For periods above 1 day, angular momentum support is not

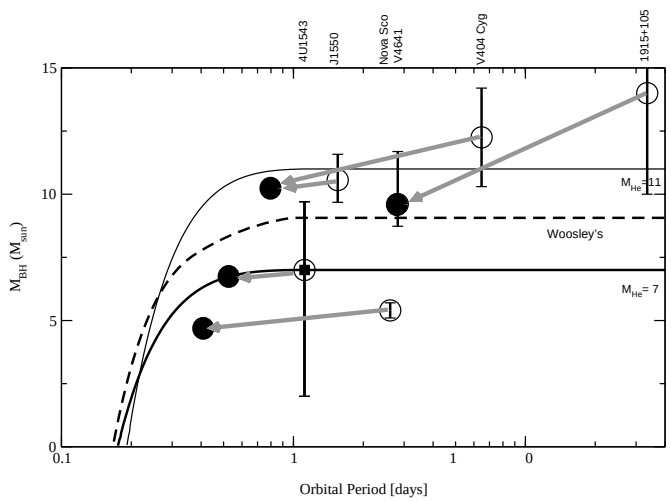

FIG. 11.—Reconstructed pre-explosion orbital period vs. black hole masses of SXTs with evolved companions. The reconstructed pre-explosion orbital periods and black hole masses are marked by filled circles, and the current locations of binaries with evolved companions are marked by open circles.

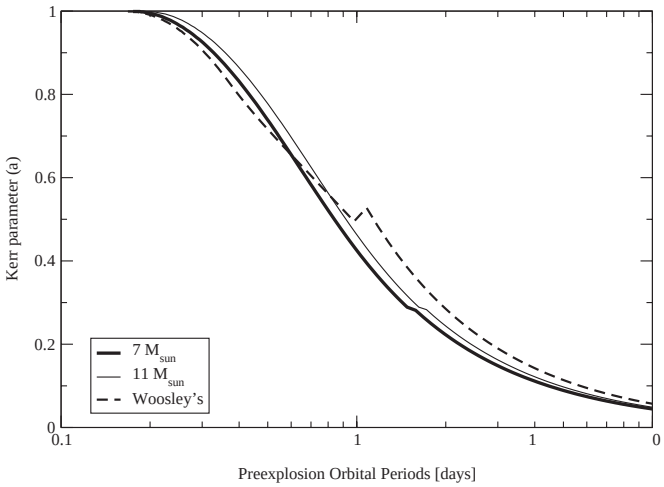

FIG. 12.—Kerr parameter of the black hole resulting from the collapse of a helium star synchronous with the orbit, as a function of orbital period. The conditions are the same as in Fig. 10, as is the meaning of the three curves. Woosley's helium core is of mass 9.15 $M_\odot$ from a ZAMS 25 $M_\odot$ star (S. E. Woosley 2001, private communication). Note that the result depends very little on the mass of the helium star or on whether we use a simple polytrope or a more sophisticated model. The plot illustrates that rapidly rotating black holes needed for powering GRBs originate only from originally short-period SXTs.

important, and the mass of the final black hole will be very close to that of the helium star and thus varies somewhat from system to system. As we can see, the reconstructed pre-explosion properties lie much closer to the theoretical predictions.

As a corollary, we find that systems with very large velocities, like Nova Sco, will be rare; at the shortest pre-explosion orbits, where much mass is ejected, the companion mass tends to be small. Then the center of mass of the binary is close to that of the helium star, which strongly limits the systemic velocity induced by the mass loss. On the other hand, for the widest systems, where the companion tends to be massive enough to allow a significant systemic velocity induced by mass loss, the mass loss itself becomes too small to induce much of a systemic velocity.

An important result for our proposed relation between SXTs and hypernovae and GRBs is shown in Figure 12. This figure shows the expected Kerr parameter of the black hole formed in our model. We see that for the short-period systems, this Kerr parameter is very large, 0.7–0.9. This means that we are justified in adding only the mass that immediately falls into the black hole, because as soon as the rapidly rotating black hole is formed, it will drive a very large energy flux in the manner described by Brown et al. (2000). This both causes a GRB and expels the leftover stellar envelope. The systems with longer orbital periods do not give rise to black holes with large Kerr parameters and thus are presumably not the sites of GRBs.

6. CONCLUSIONS

We have shown that there is an observed correlation between orbital period and black hole mass in SXTs. We have modeled this correlation as resulting from the spin of the helium star progenitor of the black hole: if the pre-explosion orbit has a short period, then the helium star spins rapidly. This means that some part of its outer envelope is

centrifugally prevented from falling into the black hole that forms at the core. This material is then expelled swiftly, leading to a black hole mass much less than the helium star mass. As the orbital period is lengthened, the centrifugal support wanes, leading to a more massive black hole. The reason for swift expulsion of material held up by a centrifugal barrier is the fact that black holes formed in our scenario naturally have high Kerr parameters (Fig. 12). This implies that they input very high energy fluxes into their surrounding medium via the Blandford-Znajek mechanism, and thus power both a GRB and the expulsion of the material that does not immediately fall in.

However, because the correlation is induced between the orbital period before explosion and the black hole mass, its manifestation in the observed correlation between black hole mass and present orbital period is weakened because of postexplosion evolution of the binaries. We therefore considered the evolution in some detail, and for a subset of the systems, we were able to reconstruct the pre-explosion orbital periods. The correlation between pre-explosion period and black hole mass (Fig. 11) is in much better agreement with our model than the original one between present period and black hole mass (Fig. 1). We developed a quantitative model for the relation between period and mass and showed that it fits the subset of reconstructible SXT orbits.

Nova Sco stands out as the most extreme case of mass loss, nearly half of the total system mass, and therefore a great widening in the orbit, which gets its period well beyond the gap between shrinking and expanding orbits. From Figure 11, we see that its black hole mass is far below the polytropic line for its $M_{\rm He} = 11\ M_\odot$ progenitor. We believe that in the case of this binary, a short central engine time of several seconds was able to furnish angular momentum and energy to the disk quickly enough to stop the infall of some of the interior matter not initially supported by centrifugal force; i.e., the angular momentum was provided in less than a dynamical time. In other words, the Blandford-Znajek mechanism that drives the GRB not only expelled the matter initially supported for a viscous time by angular momentum, but actually stopped the infall within a dynamical time.

Since we can also compute the Kerr parameters of the black holes formed via our model, we find that the short-period systems should have formed black holes with Kerr parameters in the range 0.7–0.9. This makes them prime candidates for hypernovae and GRBs and thus provides further support for our earlier study in which we posited that SXTs with black hole primaries are the descendants of GRBs. We can now also refine this statement: SXTs *with short orbital periods* before the formation of the black hole have given rise to a GRB in the past.

We would like to thank J. Orosz and S. Woosley for useful advice and information. Hans Bethe critically read the manuscript and offered helpful suggestions. We are very grateful to the referee for a number of helpful suggestions, which enabled us to improve the manuscript. In particular, the referee brought to our attention the Greiner et al. (2001) observations of 1915+105, which we could evolve as V4641 Sgr viewed at a later time. C. H. L. was in part supported by the BK21 project of the Korea Ministry of Education. We were in part supported by the US Department of Energy under grant DE-FG02-88ER40388. R. A. M. J. W. also acknowledges partial support from NASA under grant NAG5-10772.

REFERENCES

Bailyn, C. D., Jain, R. K., Coppi, P., & Orosz, J. A. 1998, ApJ, 499, 367
Beer, M., & Podsiadlowski, Ph. 2002, MNRAS, 331, 351
Bethe, H. A., & Brown, G. E. 1998, ApJ, 506, 780
Bhattacharya, D., & Van den Heuvel, E. P. J. 1991, Phys. Rep., 203, 1
Blandford, R. D., & Znajek, R. L. 1977, MNRAS, 179, 433
Brown, G. E., Heger, A., Langer, N., Lee, C.-H., Wellstein, S., & Bethe, H. A. 2001a, NewA, 6, 457
Brown, G. E., Lee, C.-H., & Bethe, H. A. 1999a, NewA, 4, 313
Brown, G. E., Lee, C.-H., Lee, H. K., & Bethe, H. A. 1999b, AIP Conf. Proc. 526, Gamma-Ray Bursts, ed. R. M. Kippen, R. S. Mallozzi, & G. J. Fishman (New York: AIP), 628
Brown, G. E., Lee, C.-H., Portegies Zwart, S. F., & Bethe, H. A. 2001b, ApJ, 547, 345
Brown, G. E., Lee, C.-H., & Tauris, T. 2001c, NewA, 6, 331
Brown, G. E., Lee, C.-H., Wijers, R. A. M. J., Lee, H. K., Israelian, G., & Bethe, H. A. 2000, NewA, 5, 191
Brown, G. E., Weingartner, J., & Wijers, R. A. M. J. 1996, ApJ, 463, 297
Eggleton, P. P. 1983, ApJ, 268, 368
Filippenko, A. V., & Chornock, R. 2001, IAU Circ., 7644, 2
Filippenko, A. V., Leonard, D. C., Matheson, T., Li, W., Moran, E. C., & Riess, A. G. 1999, PASP, 111, 969
Gelino, D. M., Harrison, T. E., & McNamara, B. J. 2001a, AJ, 122, 971
Gelino, D. M., Harrison, T. E., & Orosz, J. A. 2001b, AJ, 122, 2668
Greene, J., Bailyn, C. D., & Orosz, J. A. 2001, ApJ, 554, 1290
Greiner, J., et al. 2001, Nature, 414, 522
Harlaftis, E. T., Horne, K., & Filippenko, A. V. 1996, PASP, 108, 762
Herrero, A., Kudritzki, R. P., Gabler, R., Vilchez, J. M., & Gabler, A. 1995, A&A, 297, 556
Israelian, G., Rebolo, R., Basri, G., Casares, J., & Martin, E. L. 1999, Nature, 401, 142
Kaper, L., Camerón, A., & Barziv, O. 1999, in IAU Symp. 193, Wolf-Rayet Phenomena in Massive Stars and Starburst Galaxies, ed. K. A. van der Hucht, G. Koenigsberger, & R. J. Eenens (San Francisco: ASP), 316
Lee, H.-K., Lee, C. H., & van Putten, M. H. P. M. 2001, MNRAS, 324, 781
Li, L. X. 2000a, ApJ, 531, L111
———. 2000b, ApJ, 533, L115
———. 2000c, ApJ, 540, L17
———. 2000d, ApJ, 544, 375
———. 2002, ApJ, 567, 463
Livio, M., & Pringle, J. E. 1998, ApJ, 505, 339
MacFadyen, A. I., & Woosley, S. E. 1999, ApJ, 524, 262
McClintock, J. E., Garcia, M. R., Caldwell, N., Falco, E. E., Garnavich, P. M., & Zhao, P. 2001, ApJ, 551, L147
Nelemans, G., Tauris, T. M., & van den Heuvel, E. P. J. 1999, A&A, 352, L87
Orosz, J. A., Jain, R. K., Bailyn, C. D., McClintock, J. E., & Remillard, R. A. 1998, ApJ, 499, 375
Orosz, J. A., et al. 2001, ApJ, 555, 489
———. 2002, ApJ, 568, 845
Paczyński, B. 1998, ApJ, 494, L45
Rasio, F. A., & Livio, M. 1996, ApJ, 471, 366
Regös, E., Tout, C. A., & Wickramasinghe, D. 1998, ApJ, 509, 362
Schaller, G., Schaerer, D., Meynet, G., & Maeder, A. 1992, A&AS, 96, 269
Shahbaz, T., Bandyopadhyay, R., Charles, P. A., & Naylor, T. 1996, MNRAS, 282, 977
Shahbaz, T., Ringwald, F. A., Bunn, J. C., Naylor, T., Charles, P. A., & Casares, J. 1994, MNRAS, 271, L10
Spruit, H., & Phinney, E. S. 1998, Nature, 393, 139
Tauris, T. M., & Dewi, J. D. M. 2001, A&A, 369, 170
van Paradijs, J., Kouveliotou, C., & Wijers, R. A. M. J. 2000, ARA&A, 38, 379
van Putten, M. H. P. M. 1999, Science, 284, 115
———. 2001, Phys. Rep., 345, 1
Wagner, R. M., Foltz, C. B., Shahbaz, J., Casares, J., Charles, P. A., Starrfield, S. G., & Hewett, P. 2001, ApJ, 556, 42
Webbink, R. F. 1984, ApJ, 277, 355
Wellstein, S., & Langer, N. 1999, A&A, 350, 148
Woosley, S. E. 1993, ApJ, 405, 273